

# Quasi-Newton Methods for Unstable Partitioned Fluid-Structure Interactions

Marcel Koch (University Bonn, Germany)

## 1 Introduction

Fluid-structure interactions have applications in many engineering fields. Usually, the problem is partitioned into a fluid and a structure sub problem. Constraints on the common interface ensure the interaction between both sub problems, which are then solved separately.

The simplest method, for coupling the fluid and structure problem, is explicit coupling, which needs only one solution to each sub problem at each time step. For incompressible flows, this method is not viable, because of the *added-mass effect* [1]. The coupling becomes unstable for density ratios  $\rho_s/\rho_f$  close to 1 and stability cannot be achieved with smaller time steps.

This problem is inherent to explicit coupling methods, since the interface constraints are not satisfied. To eliminate the added-mass effect, the sub problems are coupled implicitly. Section two describes implicit coupling using quasi-Newton methods. In section three examines numerically the behavior of the quasi-Newton methods and section four gives a conclusion.

## 2 Implicit Coupling with Quasi-Newton Methods

Enforcing the interface constraints at time step  $t_{n+1}$  leads to the fixed point problem  $\mathcal{H}(x) = x$ , where  $\mathcal{H}$  depends on the coupling scheme. For example, a sequentially staggered scheme results in  $\mathcal{H} = \mathcal{S} \circ \mathcal{F}$ , where  $\mathcal{S}$  and  $\mathcal{F}$  are the solution operators to the structure and fluid problem, respectively. Currently, the coupling software MpCCI solves this fixed point equation with constant relaxation or Aitken acceleration.

Now a family of quasi-Newton methods is introduced. Therefore, the problem is written as a root finding problem  $R(x) = \mathcal{H}(x) - x$ . The generalized Broyden method [2] approximates the inverse Jacobian at iterate  $x_k$  by  $J_k \approx DR(x_k)^{-1}$ . The approximation  $J_k$  is the unique minimizer of  $\|J_k - J_{k-m}\|_F^2$  under the constraint of  $m$  secant equations  $J_k V = W$ . The difference matrices are defined by  $V = [R(x_k) - R(x_{k-m}), \dots, R(x_k) - R(x_{k-1})]$  and  $W = [x_k - x_{k-m}, \dots, x_k - x_{k-1}]$ .

The inverse residuum  $\tilde{R}(y) = y - \mathcal{H}^{-1}(y)$  has the same root as  $R(x)$  and thus can be seen as an alternative to  $R(x)$ . The approximate Jacobian  $\tilde{J}_k \approx D\tilde{R}(x_k)^{-1}$  is defined in the same manner as  $J_k$ . Special care must be taken, when computing the next iterate. Since  $\mathcal{H}^{-1}$  is not available, the inverse residuum cannot be evaluated directly. Instead, with the new iterate  $y_{k+1} = \mathcal{H}(x_{k+1})$ , where  $x_{k+1} = y_k - \tilde{J}_k \tilde{R}(y_k)$  is an intermediate update, the inverse residuum is simply  $\tilde{R}(y_{k+1}) = R(x_{k+1})$ . This approach is called inverse generalized Broyden method. Both algorithms are summarized in the following.

<i>Generalized Broyden Method</i>	<i>Inverse Generalized Broyden Method</i>
<b>Input:</b> $\mathcal{H}, x_0, J_0, m$	<b>Input:</b> $\mathcal{H}, x_0, \tilde{J}_0, m$
<b>Output:</b> $x_*, J_*$	<b>Output:</b> $x_*, \tilde{J}_*$
<b>for</b> $k = 0, 1, \dots$ <b>until</b> converged	<b>for</b> $k = 0, 1, \dots$ <b>until</b> converged
$y_k = \mathcal{H}(x_k)$	$y_k = \mathcal{H}(x_k)$
$R_k = y_k - x_k$	$R_k = y_k - x_k$
$V = [\Delta R_{k-m}, \dots, \Delta R_{k-1}]$	$V = [\Delta R_{k-m}, \dots, \Delta R_{k-1}]$
$W = [\Delta x_{k-m}, \dots, \Delta x_{k-1}]$	$\tilde{W} = [\Delta y_{k-m}, \dots, \Delta y_{k-1}]$
$\alpha = \operatorname{argmin}_{\beta \in \mathbb{R}^d} \ \mathcal{V}\beta + R_k\ $	$\alpha = \operatorname{argmin}_{\beta \in \mathbb{R}^d} \ \mathcal{V}\beta + R_k\ $
$x_{k+1} = x_k - J_{k-m} R_k - (W - J_{k-m} V)\alpha$	$x_{k+1} = y_k - \tilde{J}_{k-m} R_k - (\tilde{W} - \tilde{J}_{k-m} V)\alpha$
$J_{k+1} = J_{k-m} + (W - J_{k-m} V)(V^T V)^{-1} V^T$	$\tilde{J}_{k+1} = \tilde{J}_{k-m} + (\tilde{W} - \tilde{J}_{k-m} V)(V^T V)^{-1} V^T$

Cases of special interest are  $m = 1$  and  $m = \infty$ . The choice  $m = 1$  results in the widely known Broyden method, which minimizes  $\|J_{k+1} - J_k\|_F^2$ . In the other interesting case  $m = \infty$ , the generalized Broyden method equals the Anderson mixing, if the initial matrix is chosen as  $J_0 = -\beta I$ . Since the new approximation  $J_{k+1}$  is only needed if  $k > m$ , the Anderson mixing never computes  $J_{k+1}$ .

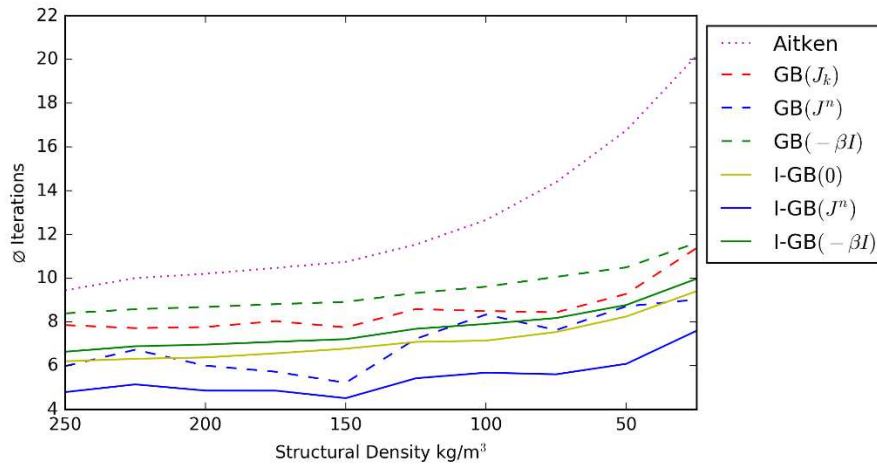


Fig. 1

Mean number of iterations to achieve  $\frac{\|R_k\|}{\|x_k\| + \|y_k\|} < 10^{-7}$  with different structural densities.

The fixed point problem  $\mathcal{H}(x) = x$  is part of a time stepping method. Therefore, it is reasonable to reuse information from the previous time step. This is achieved by setting  $J_0 = J_*^n$ , where  $J_*^n$  is the converged approximation of the Jacobian for the time step  $t_n$ . Therefore, the matrix  $J_*^n$  must be computed explicitly either at the end of the current time step or at the beginning. The corresponding inverse generalized Broyden method is known as the *multi-vector update quasi-Newton (MVQN)* method, introduced in [3].

For the inverse generalized Broyden method, the choice  $m = \infty$  and  $J_0 = 0$  is possible, after the first iteration. This is the *least square quasi-Newton* method, developed by Haelterman and Degroote [4]. The related generalized Broyden method and the inverse equivalent of Broyden's method are both unstable, since they create linear dependent iterates.

The methods are characterized by the number secant equation, the initial matrix guess and the type of fixed point problem. The quasi-Newton method considered here are the following:

	GB( $J_k$ )	GB( $-\beta I$ )	I-GB( $-\beta I$ )	GB( $J_*^n$ )	I-GB( $J_*^n$ )	I-GB(0)
$m$	1	$\infty$	$\infty$	$\infty$	$\infty$	$\infty$
$J_0$	$J_*^n$	$-\beta I$	$-\beta I$	$J_*^n$	$J_*^n$	0
$\mathcal{H}$	$\mathcal{H}$	$\mathcal{H}$	$\mathcal{H}^{-1}$	$\mathcal{H}$	$\mathcal{H}^{-1}$	$\mathcal{H}^{-1}$

Only the Broyden method GB( $J_k$ ) requires to update the approximation in each quasi-Newton iteration. The Anderson variants with  $J_0 \in \{-\beta I, 0\}$  do not construct the matrices  $J_k$  explicitly, since the matrix vector multiplication is done using only the difference matrices  $V, W$ . Additionally, the methods GB( $J_*^n$ ) and I-GB( $J_*^n$ ) must compute the approximate Jacobian from the previous time step in the first iteration associated with a new time step.

### 3 Numerical Investigation

In the following numerical examples, the commercial software packages ABAQUS and FLUENT are employed to solve the structure and fluid sub problem respectively. The coupling of the two solvers is done by the software MpCCI. For the following examples, implicit coupling with the staggered sequential scheme  $\mathcal{H} = \mathcal{F} \circ \mathcal{S}$  has been applied.

The first example is a driven cavity model with flexible bottom, see figure 2. The fluid density is set to  $\rho_f = 1\text{kg/m}^3$ , while the structural density ranges from  $\rho_s = 25, \dots, 250\text{kg/m}^3$ . In [1] the authors show that explicit coupling diverges for structural densities lower than  $321\text{kg/m}^3$ . The implicit coupling with quasi-Newton methods results in a stable solution for structural densities ranging down to  $25\text{kg/m}^3$ . Figure 1 depicts the mean number of iterations for each method to achieve a relative residual less than  $10^{-7}$ .

The first interesting observation is that the lower structural density still has negatives effects on the simulation. All methods require a greater number of iterations to converge for lower structural densities. This coincides with the results of [5], where the authors show the influence of the structural density on the convergence of constant relaxation to solve the fixed point problem. The negligible influence of the time step size on the convergence will be shown in the presentation.

Secondly, all quasi-Newton methods converge faster than the Aitken acceleration, for the lowest density ratio, they need at worst halve the amount of iterations required by the Aitken method. Of these quasi-Newton method, the inverse methods outperform their standard generalized Broyden variants.

Furthermore, the best performance has the inverse Anderson mixing type with initial guess matrix from the previous time step. In contrast, the I-GB( $-\beta I$ ) method, which is equivalent, except it discards all information from the time steps before, needs around two more iterations to converge. This indicates that information, from the previous time steps, has a significant influence on the convergence.

The second example is the benchmark proposed by Turek et al. [6], see figure 3. Both the fluid and structure density equal  $\rho = 1000\text{kg/m}^3$ , implying strong influences from the added-mass effect. Explicit coupling with a time step size of  $\Delta t = 0.001\text{s}$  diverges after less than ten time steps. The implicit coupling variant results in a stable simulation over the interval  $[0,10\text{s}]$ , for all quasi-Newton methods.

The following table shows the mean number of quasi-Newton iterations required until convergence with a relative residuum of less than  $10^{-7}$ . The Aitken acceleration is again used as reference. Additionally, the maximal computational time for one quasi-Newton iteration and the total time spend on quasi-Newton iterations are displayed, without the evaluation of  $\mathcal{H}$ .

<i>Method</i>	$\emptyset$ Iterations	<i>max</i> $\Delta t$	$\Sigma \Delta t$
Aitken	24,98	-	-
GB( $J_k$ )	8,77	1.59 ms	53.48 s
GB( $J_*^n$ )	11,48	1697.08 ms	61.17 s
GB( $-\beta I$ )	14,71	0.77 ms	26.99 s
I-GB( $-\beta I$ )	10,63	0.57 ms	21.49 s
I-GB( $J_*^n$ )	6,63	356.03 ms	24.86 s
I-GB(0)	9,86	0.41 ms	17.67 s

Once again, this table show that the quasi-Newton are superior to the currently implemented Aitken acceleration. Furthermore, the inverse methods converge faster than their counterparts. This indicates that the inverse generalized Broyden method is better suited to solve fluid-structure interactions. The I-GB( $J_*^n$ ) method outperforms all other methods, similar to the first example. In contrast to the driven cavity example, the usual Broyden method has the second lowest mean number of iterations. The lower number of iterations result from the higher number of time steps for this example, because Broyden's method benefits for more time steps from the reuse of information.

The maximal computational effort for one quasi-Newton iteration is the lowest for the Anderson methods without information from earlier time steps, since they do not rely on dense square matrices. These methods only rely on the solution to the least square problem  $\|V\beta + R_k\|$  and multiplication with the matrices  $V$  and  $W$ , where both have a low number of columns. Reusing previous approximation requires the dense and square formulation of  $J_*^n$  and thus they take at least twice the computational effort.

The extremely high computational cost of the GB( $J_*^n$ ) and I-GB( $J_*^n$ ) variant stems from the overuse of information from earlier time steps. Then, the resulting initial guess  $J_*^n$  does not lead to a suitable approximation of the Jacobian in the current time step. Instead, the methods are restarted with  $J_0 = -\beta I$ . At first, this slows down the convergence, but after a few time steps the previous convergence rate is attained. It becomes evident from the overall computational effort that these restarts happen rarely.

## 4 Conclusions

This paper introduced the inverse generalized Broyden method for the solution of fixed point problems. For a selection of quasi-Newton, the influence of the added-mass effect was considered. Besides, their performance was compared to the Aitken acceleration, currently implemented in MpCCI. Across the board, all tested quasi-Newton methods outperformed the Aitken acceleration by a factor of 2 to 4 for density ratios close to one. Furthermore, the inverse generalized Broyden methods converged faster than their respective generalized Broyden counterparts, making them favorable for the simulation of fluid-structure interaction. Although all implicit coupling simulations were stable for all density ratios, remnants of the added-mass effect were visible through the slower convergence with decreasing density ratio.

## 5 References

- [1] Förster C., Wall W., Ramm E.: "Artificial added mass instabilities in sequential staggered coupling of nonlinear structures and incompressible viscous flows." *Computer methods in applied mechanics and engineering*, 2007
- [2] Fang H. R., Saad Y.: "Two classes of multiseant methods for nonlinear acceleration." *Numerical Linear Algebra with Applications*, 2009
- [3] Bogaers A. E. J., Kok S., Reddy B. D., Franz T.: "Quasi-Newton methods for implicit black-box FSI coupling." *Computer Methods in Applied Mechanics and Engineering*, 2014
- [4] Haelterman R., Degroote J., Van Heule D., Vierendeels J.: "The quasi-Newton least squares method: a new and fast secant method analyzed for linear systems." *SIAM Journal on numerical analysis*, 2009
- [5] Causin P., Gerbeau J. F., Nobile F.: "Added-mass effect in the design of partitioned algorithms for fluid–structure problems." *Computer methods in applied mechanics and engineering*, 2005
- [6] Turek S., Hron J.: "Proposal for numerical benchmarking of fluid-structure interaction between an elastic object and laminar incompressible flow." *Fluid-structure interaction*, 2006

## 6 Example geometry

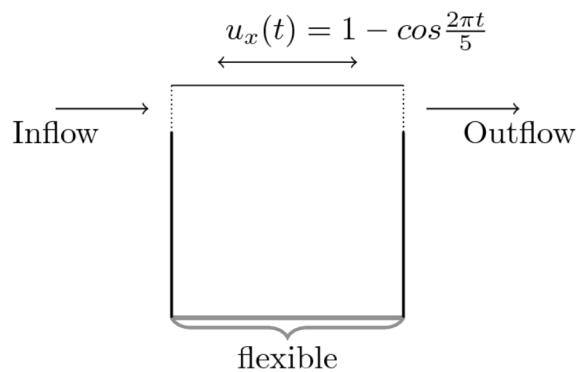


Fig. 2

Driven cavity model with flexible bottom. The viscosity is set to  $\nu_f = 0.01 \text{ m}^2/\text{s}$ , Young's modulus to  $E = 250 \text{ N/m}^2$  and the Poisson's ratio to  $\nu_s = 0$ .

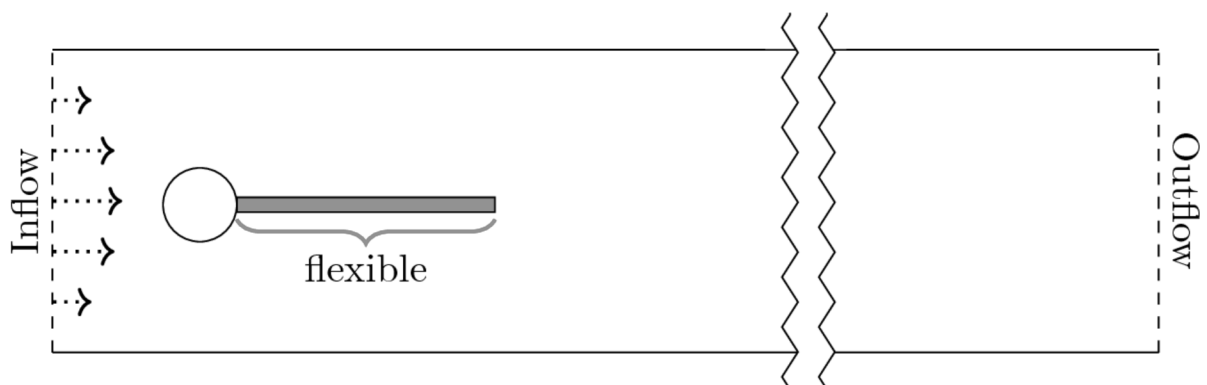


Fig. 3

Flow around a cylinder with a flexible beam. The fluid viscosity is set to  $\nu_f = 10^{-3} \text{ m}^2/\text{s}$ , the Young's modulus to  $E = 5.6 \cdot 10^6 \text{ N/m}^2$  and the Poisson's ratio to  $\nu_s = 0.4$ .